Frontiers in Bioscience Landmark

Front. Biosci. (Landmark Ed) **2026**; 31(11): 55654
https://doi.org/10.31083/FBL55654

Original Research

MEX3C Serves as a Critical Molecule in XPO1-Mediated Chemotherapy Resistance in SCLC

Peiyan Zhao[1,2], Shuang Zhang[3], Xinyue Wang[1,2], Heran Cui[1,2], Yuanhua Lu[4], Hui Li[1,2,*], Haifeng Liu[1,2,*]

[1]Translational Oncology Research Lab, Jilin Cancer Hospital, 130000 Changchun, Jilin, China
[2]Jilin Provincial Key Laboratory of Molecular Diagnostics for Malignant Tumor, Jilin Cancer Hospital, 130000 Changchun, Jilin, China
[3]Department of Internal Medicine IV, High-Tech Zone Campus, Jilin Cancer Hospital, 130000 Changchun, Jilin, China
[4]Postdoctoral Research Workstation, Jilin Cancer Hospital, 130000 Changchun, Jilin, China
*Correspondence: lihui0620@csco.org.cn (Hui Li); hflydw@163.com (Haifeng Liu)
Academic Editor: Graham Pawelec
Submitted: 6 July 2026 Revised: 31 August 2026 Accepted: 30 September 2026 Published: 13 November 2026

Abstract

Background: Exportin-1 (XPO1) is an export receptor responsible for nucleocytoplasmic transport and can function as an oncogenic driver in human cancers. However, its role in refractory small-cell lung cancer (SCLC) remains poorly understood. In this study, we used publicly available SCLC patient datasets to analyze the relationship between XPO1 expression and chemotherapy resistance. **Methods:** Parental and chemotherapy-resistant SCLC cell lines were used to investigate the association between XPO1 and chemoresistance. Transcriptomic and proteomic analyses were performed to identify key molecules involved in SCLC chemoresistance. Data from public databases, together with immunofluorescence, co-immunoprecipitation, Western blotting, and cell viability assays, were used to investigate associations and interactions between XPO1 and MEX3C, as well as the effects of combined inhibition. **Results:** XPO1 expression was elevated in chemotherapy-resistant SCLC cells. Patients with SCLC and low XPO1 expression showed trends toward prolonged overall and progression-free survival, although these associations did not reach statistical significance. Proteomic analysis identified the shuttling protein MEX3C as a potential regulator of chemoresistance, with MEX3C expression positively correlated with XPO1 expression. MEX3C and XPO1 co-localized and physically interacted within the nucleus of SCLC cells. XPO1 knockdown reduced MEX3C expression. XPO1 inhibitors significantly suppressed SCLC cell growth, while combined treatment with an XPO1 inhibitor and MEX3C knockdown further inhibited the proliferation of chemotherapy-resistant SCLC cells. **Conclusions:** These findings suggest a functional relationship between XPO1 and MEX3C in chemotherapy-resistant SCLC and support further investigation of combined targeting of XPO1 and MEX3C as a potential therapeutic strategy.

Keywords: small cell lung carcinoma; active transport; drug therapy; cell nucleus

1. Introduction

The maintenance of cellular homeostasis relies heavily on the precise spatiotemporal regulation of proteins. Chromosome Region Maintenance 1 (CRM1), also known as exportin-1 (XPO1), is the primary nuclear export receptor responsible for shuttling hundreds of cargo proteins, including major tumor suppressors such as p53, BRCA1, Forkhead box O (FOXO), and IkappaB (IκB), from the nucleus to the cytoplasm [1,2]. This transport system is frequently hijacked by malignant cells. Overexpression of XPO1 has been documented across a wide spectrum of hematological and solid malignancies, leading to aberrant cytoplasmic mislocalization of tumor suppressors and growth regulatory proteins. This process effectively neutralizes their anti-proliferative and pro-apoptotic functions, thereby promoting uncontrolled cell cycle progression, genomic instability, and evasion of apoptosis [3,4]. High XPO1 expression levels are strongly correlated with aggressive clinicopathological features and poor prognosis, establishing XPO1 as a validated anti-cancer target [5]. The clinical translation of this concept has been realized with the development of selective inhibitors of nuclear export (SINE), such as Selinexor, which have demonstrated efficacy by trapping tumor suppressors in the nucleus. The Food and Drug Administration (FDA) has approved Selinexor for relapsed/refractory multiple myeloma and diffuse large B-cell lymphoma [6,7].

Among solid tumors, small-cell lung cancer (SCLC) represents an exceptionally aggressive and lethal malignancy characterized by rapid growth, early metastasis, and the absence of targetable driver mutations [8,9]. Despite initial high sensitivity to platinum-based chemotherapy, resistance almost invariably develops within months, leading to disease relapse and a dismal 5-year survival rate of <7% [9]. Recent evidence positions XPO1 as a critical dependency in SCLC. Studies have reported that XPO1 is strongly overexpressed in SCLC patient specimens and cell lines compared to normal lung tissue [10]. Mechanistically, XPO1 drives SCLC progression by promoting the nuclear exclusion of key tumor suppressors. For instance,

Copyright: © 2026 The Author(s). Published by IMR Press.
This is an open access article under the CC BY 4.0 license.

Publisher's Note: IMR Press stays neutral with regard to jurisdictional claims in published maps and institutional affiliations.

XPO1-mediated export of Forkhead box O3a (FOXO3a), a transcription factor governing pro-apoptotic genes, has been identified as a mechanism of resistance to poly ADP-ribose polymerase (PARP) inhibitors in SCLC [11]. This phenomenon was found to be reversible upon XPO1 knockdown. Furthermore, SCLC is characterized by a high incidence of TP53 and RB1 co-inactivation, a genetic context that paradoxically increases XPO1 transcriptional activity via E2F1, creating a synthetic lethal dependency on XPO1 function [12]. Notably, a recent study reported a novel SCLC subtype with high expression of histone deacetylase 7 (HDAC7) that exhibited poor prognosis. HDAC7 activates the β-catenin/c-Myc axis to upregulate XPO1 expression. These aggressive cells demonstrated marked sensitivity to Selinexor, suggesting that inhibition of XPO1 may represent a tailored strategy for specific SCLC subsets [10].

The role of XPO1 in therapeutic resistance extends beyond SCLC and represents a more generalized mechanism of treatment failure across different cancer types. Chemotherapy and targeted therapy exert selective pressures that often upregulate XPO1 activity. In colorectal cancer, XPO1 mutations drive resistance to Topoisomerase I inhibitors by enhancing DNA repair pathways, a vulnerability that may be exploited by Selinexor [13]. Similarly, in TP53-mutated myeloid malignancies, treatment with DNA methyltransferase inhibitors upregulates XPO1, leading to the cytoplasmic shuttling and inactivation of p53 and thus driving acquired resistance. However, this adaptive response renders malignant cells susceptible to XPO1 inhibitors [14]. In aggressive lymphomas, XPO1 selectively exports mRNAs encoding genome maintenance proteins via RNA-binding proteins to promote chemoresistance [12]. Despite the growing interest in XPO1 as a therapeutic target in other cancer types, its role in SCLC remains largely unexplored.

In the present study, we utilized database information from SCLC patients to analyze the relationship between XPO1 expression level and patient survival. We also used parental and chemotherapy-resistant SCLC cell lines to investigate the association between XPO1 expression and chemoresistance. Furthermore, transcriptomic and proteomic analyses identified MEX3C as a key molecule through which XPO1 regulates chemotherapy resistance. Using information extracted from SCLC patient and cell line databases, along with various cellular analyses, we examined the correlation between XPO1 and MEX3C expression, as well as their functional interaction. Additionally, we reveal a synergistic effect of combined XPO1 and MEX3C inhibition in SCLC. Collectively, these findings provide novel information on the key upstream and downstream regulatory genes of XPO1 in SCLC, the screening of synergistic therapeutic targets, and the development of individualized precision treatment strategies.

2. Materials and Methods

2.1 Analysis of Transcriptome Data From SCLC Databases

The RNA-seq data and clinical information from 81 SCLC tumor tissue samples reported by George et al. [15] were downloaded from the cBioPortal database (http://www.cbioportal.org). Survival analysis was performed on 77 out of the 81 SCLC patients, since four samples lacked complete overall-survival follow-up information. The relationship between MEX3C and XPO1 was analyzed from Cancer Cell Line Encyclopedia using SclcCellMinerCDB (https://discover.nci.nih.gov/SclcCellMinerCDB/) and RNA-seq data from tumor tissue using cBioPortal, respectively.

2.2 Cell Culture

The human SCLC cell line SCLC-21H (21H) was purchased from Zhong Qiao Xin Zhou Biotechnology company, while the SCLC cell lines NCI-H196 (H196), NCI-H69 (H69), and NCI-H2141 (H2141) were obtained from Procell Life Science &Technology Co., Ltd. All cell lines used in this study were authenticated by short tandem repeat (STR) profiling and tested negative for mycoplasma contamination. The human SCLC cell line H82, its chemotherapy-resistant derivative (H82R), as well as the H526 cell line and its chemotherapy-resistant derivative (H526R) were generously provided by Prof. Hongbin Ji (University of Chinese Academy of Sciences). Cells were cultured in RPMI-1640 medium (Sigma-Aldrich, St. Louis, MO, USA) supplemented with 10% (v/v) fetal bovine serum (FBS) (Vivacell, Shanghai, China) and 100 U/mL of penicillin and 100 µg/mL of streptomycin (Biological Industries, Kibbutz Beit Haemek, Israel). Cells were maintained in a humidified incubator at 37 ℃ and 5% CO_2.

2.3 Drug Treatment

SCLC cells were seeded into 96-well plates at a density of 5000 cells per well and treated with increasing concentrations of chemotherapeutic agents as follows: cisplatin (0.07–20 µg/mL) and etoposide (0.12–30 µg/mL). Cells were also treated with the XPO1 inhibitor Selinexor (HY-17536, MCE), WJ01075, or WJ01024 at concentrations ranging from 0.07–20 µM.

2.4 Cell Viability Assay

Cell viability was determined with Cell Counting Kit-8 (CCK-8, catalogue number C0038, Beyotime). Briefly, CCK-8 reagent was added to each well at a volume equal to 10% of the culture medium, and cells were incubated for 1 h. The absorbance measured at 450 nm was used to evaluate cell viability using the formula: $(OD_{sample} - OD_{spontaneous}) / (OD_{control} - OD_{spontaneous}) \times 100\%$.

2.5 Western Blotting

Western blotting was conducted as described previously [16]. Briefly, SCLC cells were lysed in radioim-

munoprecipitation assay (RIPA) buffer containing 1 mM phenylmethylsulphonyl fluoride (PMSF) and then centrifuged at 15,000 ×g for 15 min at 4 °C. The supernatant was collected and the protein concentration quantified using Enhanced BCA Protein Assay Kit (P0010, Beyotime). Equal amounts of protein were fractionated by sodium dodecyl sulfate polyacrylamide gel electrophoresis (SDS-PAGE) and subsequently transferred to polyvinylidene fluoride membranes (Millipore, Billerica, MA, USA). These were blocked with skimmed milk and then incubated overnight at 4 °C with different primary antibodies in buffer containing 5% skimmed milk. After washing three times with tris-buffered saline (TBS) containing 0.05% Tween-20, the membranes were incubated with a secondary antibody for 1 h at room temperature and then washed again three times. Protein bands were visualized using chemiluminescence (P0018AM, Beyotime) and analyzed with ImageJ software (version 1.8.0) (National Institutes of Health, Bethesda, Maryland, USA). The primary antibodies were against glyceraldehyde-3-phosphate dehydrogenase (GAPDH) (AP0066, Bioworld, 1:10,000), XPO1 (sc-374124, Santa Cruz, 1:100), and MEX3C (NBP1-76341, NOVUS, 1:1000), while the secondary antibody was horseradish peroxidase-conjugated goat anti-rabbit immunoglobulin G (IgG) (RM3002, Ray Antibody Biotech, 1:10,000) and goat anti-mouse IgG (RM3001, Ray Antibody Biotech, 1:10,000).

2.6 RNA Sequencing

Total RNA was extracted from SCLC cells using TRIzol reagent and subsequently used for RNA-seq (BGI, Wuhan, China). Three parallel replicates were prepared for each group. In brief, mRNAs were first enriched by oligo(dT) magnetic beads, and the enriched mRNAs were then fragmented and synthesized to cDNA. The cDNA fragments were end-repaired and adenylated at the 3′ ends. Universal adapters were ligated to the cDNA fragments, followed by polymerase chain reaction (PCR) amplification. The library products were sequenced by BGISEQ. Raw data were filtered using SOAPnuke (v1.5.6), and clean reads were aligned to the reference genome (GCF_000001405.39_GRCh38.p13) by HISAT. Bowtie2Clean was used to align clean reads to the reference gene sequence. Pathway analysis for differentially expressed genes (DEGs), which were screened with the threshold of $|\log_2(\text{fold-change})| \geq 1.5$, was performed on the Dr. Tom network platform (http://biosys.bgi.com/).

2.7 Nuclear Protein Isolation

Nuclear and cytoplasmic proteins were extracted from SCLC cells using a Nuclear and Cytoplasmic Protein Extraction Kit (P0027, Beyotime) according to the manufacturer's instructions. Briefly, cell pellets were resuspended in cytoplasmic protein extraction reagent A supplemented with PMSF, followed by vigorous vortexing at maximum speed for 5 seconds to completely disperse the cell pellets. The samples were then incubated on ice for 15 minutes. Cytoplasmic protein extraction reagent B was added, and the samples were vigorously vortexed at maximum speed for 5 seconds, followed by incubation on ice for 1 minute. After an additional 5-second vigorous vortexing, the samples were centrifuged at 12,000 ×g for 5 minutes at 4 °C. The supernatant was completely aspirated, and the pellet was resuspended in nuclear protein extraction reagent supplemented with PMSF. The samples were vigorously vortexed at maximum speed for 30 seconds to fully disperse the pellet, then placed on ice. This vortexing step was repeated every 2 minutes for a total of 30 minutes. The samples were then centrifuged at 12,000 ×g for 10 minutes at 4 °C. The supernatant (nuclear protein extract) was immediately transferred to a pre-chilled Eppendorf tube and used for subsequent protein sequencing.

2.8 iTRAQ Proteomic Analysis

A total of 200 µg protein was denatured, reduced with 5 mM tris(2-carboxyethyl)phosphine (TCEP), alkylated with 10 mM S-methyl methanethiosulfonate (MMTS), then digested with trypsin (1:50, w/w) at 37 °C overnight. For isobaric tags for relative and absolute quantitation (iTRAQ) labelling, each experimental group contained 3 biological replicates. Tryptic peptides (200 µg) derived from each sample were labelled with iTRAQ 8-plex reagents (Applied Biosystems) as per the standard operating procedure from BGI Genomics Co., Ltd., then quenched, pooled, desalted, and dried. The iTRAQ tag assignment and sample-tag correspondence are summarized: parental replicates were labelled with tags 113–115, and resistant replicates were labelled with tags 116–118. Labelled peptides were pooled and subjected to liquid chromatography-tandem mass spectrometry (LC-MS/MS) analysis as described above. The dried peptides were fractionated by high-performance liquid chromatography (HPLC) (ERLIC column) into 20 fractions and reconstituted for LC-MS/MS (nano-bore C18 column, Q-Exactive/Q Star® Elite). The raw data were converted to MGF format, and protein identification/quantification was performed using Mascot 2.3.02 (false discovery rate [FDR] ≤1%) and IQuant (Huada). Differentially expressed proteins (DEPs) were defined as FC >1.2 and Q <0.05. Quality control samples were used to evaluate stability (CV <20%, principal component analysis [PCA] clustering). The pathway analysis for DEPs was performed on the Dr. Tom network platform (http://biosys.bgi.com/).

2.9 Transfection of Short Hairpin RNAs

Short hairpin RNAs (shRNAs) for human *XPO1* and human *MEX3C* were obtained from Genechem. ShRNAs targeting the *XPO1* gene sequence (*XPO1*-1: CCTCACCTACAAGATGCTCAA; *XPO1*-2: GCTCAAGAAGTACTGACACAT; *XPO1*-3: CCATTGTAAAGCGACTTCAAA), the *MEX3C* gene sequence (CCATGCG-

TACAGGAAACTATA), and the negative control (TTCTCCGAACGTGTCACGT) were cloned into the GV493 plasmid expression vector. Cell transfection was performed strictly according to the manufacturer's instructions for Lipofectamine 2000 (ThermoFisher). Briefly, H82 (for sh*XPO1*) or H82R (for sh*MEX3C*) cells were seeded 24 h in advance, and transfection was initiated when cell confluence reached 60%. Plasmid DNA was mixed with Lipofectamine 2000 at a mass-to-volume ratio of 1:2, with 5 μg plasmid per well. DNA-lipid mixtures were diluted in serum-free Opti-MEM medium (31985062, Gibco) and incubated at room temperature for 20 min to form transfection complexes. Subsequently, the mixture was added dropwise to the cell culture plate, and cells were incubated in a humidified incubator for 48 h.

2.10 Immunofluorescence Assay

SCLC cells were collected by low-speed centrifugation at 800 rpm for 5 minutes and washed twice with phosphate-buffered saline (PBS). They were then added to polylysine-coated coverslips, allowed to adhere statically, fixed with 4% paraformaldehyde for 20 minutes at room temperature, and washed three times with PBS (5 minutes each). Permeabilization was performed with 0.5% Triton X-100 for 10 minutes at room temperature, followed by three washes with PBS. The cells were blocked with 5% bovine serum albumin (BSA) for 60 minutes at room temperature and then washed. The coverslips were incubated overnight at 4 °C with primary antibodies diluted as follows: XPO1 (CRM1) antibody (A-7) (sc-374124, Santa Cruz) at 1:50; and MEX3C antibody (NBP1-76341, NOVUS) at 1:100. The following day, the cells were washed three times with PBS (5 minutes each) and secondary antibodies were applied as follows: goat anti-rabbit IgG (H+L) (min X Hu Sr Prot) (Alexa Fluor® 647 Conjugate) (S0B4051, STARTER) at 1:500 and Fluorescein (FITC)-conjugated goat anti-mouse IgG (H+L) (SA00003-1, Proteintech) at 1:100. The cells were incubated with secondary antibodies for 1 h at room temperature in the dark, followed by three washes with PBS in the dark. Nuclei were counterstained with 4′,6-diamidino-2-phenylindole (DAPI) (NG0271, Beyotime) for 5 minutes, and excess dye was removed by washing with PBS. The coverslips were then mounted, and fluorescence images were acquired using a fluorescence microscope.

2.11 HA-Tagged Protein Co-Immunoprecipitation

Recombinant overexpression plasmids were generated, in which MEX3C was tagged with FLAG and XPO1 was tagged with hemagglutinin (HA). Normal mouse-derived IgG was included as the negative-control immunoprecipitation sample, and anti-HA antibody was utilized as the bait for co-immunoprecipitation (Co-IP). HA-tagged protein Co-IP was performed using a commercial kit (P2206S, Beyotime) as per the manufacturer's protocol. H82 cells were lysed in buffer containing a protease inhibitor cocktail (100:1). After centrifugation (10,000 ×g, 5 min, 4 °C), the supernatant was incubated with agarose gel overnight at 4 °C on a rotator. The gel was washed three times with lysis buffer containing inhibitors (6000 ×g, 30 s each, 4 °C), then eluted with 2× SDS-PAGE loading buffer at 95 °C for 5 min. The eluted proteins were analyzed by Western blotting using anti-mAb antibody (AE105, ABclonal) diluted 1:10,000.

2.12 Statistical Analysis

All statistical analyses were conducted with SPSS 27.0 and GraphPad Prism 8.0 software. The Shapiro-Wilk test was adopted to test the normality of all continuous measurement data before statistical analysis. For normally distributed continuous variables, the results were presented as means ± standard deviations. One-way analysis of variance (ANOVA) with post-hoc multiple comparisons was used for comparisons among three or more groups, while Student's two-tailed independent-samples *t*-test was applied to compare two groups. A two-tailed p-value < 0.05 was defined as statistically significant. A four-parameter logistic model was fitted to generate cell proliferation inhibition curves, and the extra sum-of-squares F test was adopted to compare LogIC50 values across groups for evaluating cellular drug sensitivity. Survival curves were plotted via the Kaplan–Meier method, and intergroup survival differences were compared using the log-rank test. Two-way repeated-measures ANOVA with Bonferroni correction for multiple comparisons was performed to analyze the proliferative viability of H82R cells treated with three distinct drug regimens at multiple time points. All cellular experiments were repeated at least three times, and only representative images are presented for Western blotting and immunofluorescence assays.

3. Results

3.1 High XPO1 Expression in SCLC is Associated With Chemotherapy Resistance

Survival data for SCLC patients in the published article [15] (N = 77) were analyzed by the Kaplan–Meier method. Although statistical significance was not reached, patients with low XPO1 expression showed trends toward longer overall survival (OS) and progression-free survival (PFS) compared to those with high XPO1 expression (OS: HR, 0.65, 95% CI: 0.37–1.16, log-rank $p = 0.1363$; PFS: HR, 0.5, 95% CI: 0.225–1.12, log-rank $p = 0.0895$) (Fig. 1A,B, Ref. [15]). To further investigate the role of XPO1 in chemotherapy resistance, we utilized parental H82 and H526 cell lines, as well as their chemotherapy-resistant derivatives (H82R and H526R). First, we confirmed that H82R and H526R cells exhibited reduced sensitivity to cisplatin and etoposide compared to their respective parental cells (Fig. 1C). Subsequently, we found that H82R cells showed significantly higher XPO1 expression levels than

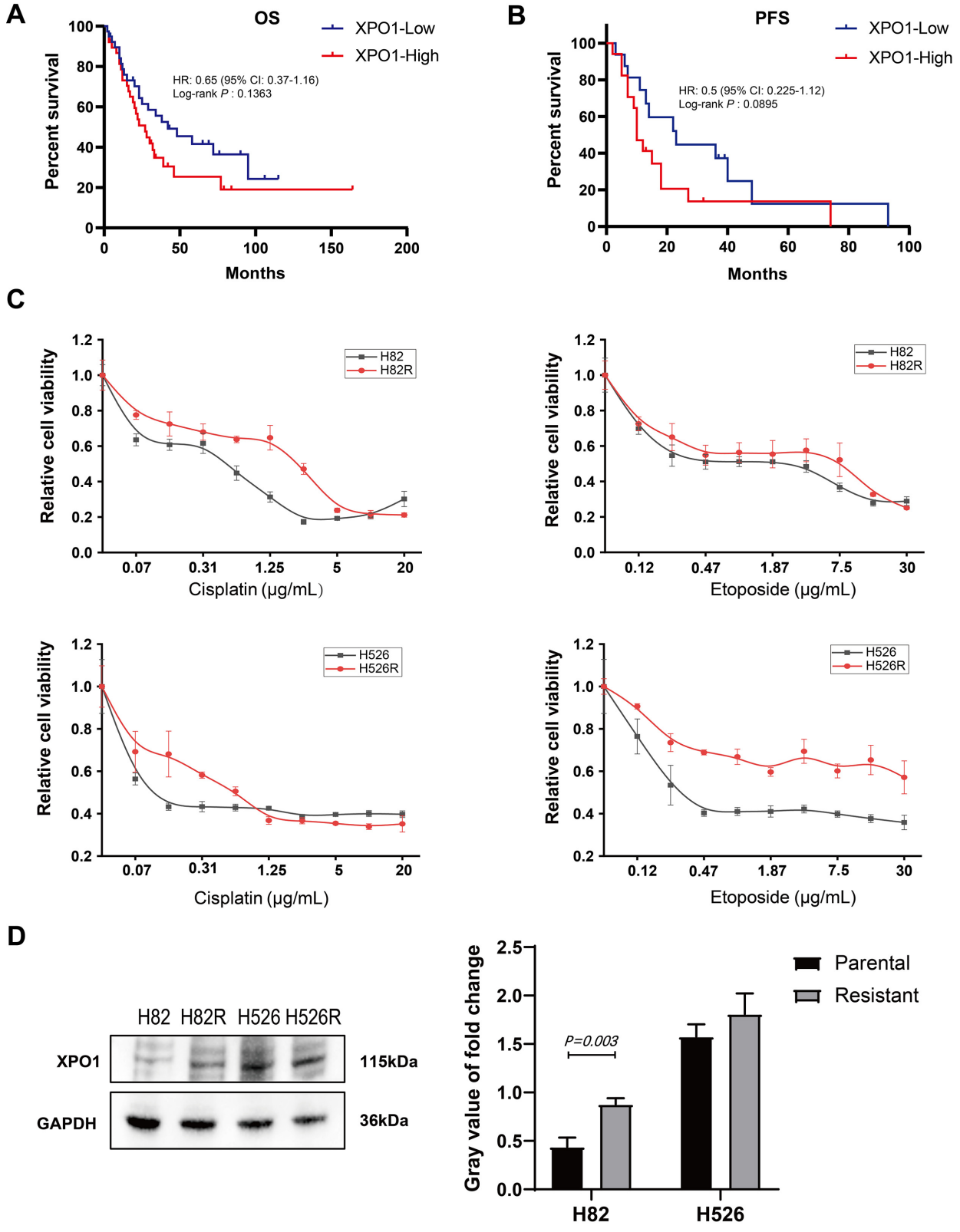


Fig. 1. Relationship between expression of XPO1 and prognosis of SCLC patients or chemoresistance of SCLC cells. (A) Overall survival and (B) progression-free survival of SCLC patients from the published article (George et al., 2015 [15]) (N = 77). Patient groups with high or low XPO1 expression were analyzed. (C) The relative cell viability of H82 and H82R cells treated with cisplatin or etoposide was measured by CCK-8 assay ($n = 3$ for biological replicates). (D) Protein levels of XPO1 and GAPDH in H82, H82R, H526 and H526R cells were assessed by Western blotting ($n = 3$ for biological replicates). XPO1, exportin-1; SCLC, small-cell lung cancer; CCK-8, Cell Counting Kit 8; GAPDH, glyceraldehyde-3-phosphate dehydrogenase; HR, Hazard Ratio; CI, Confidence Interval.

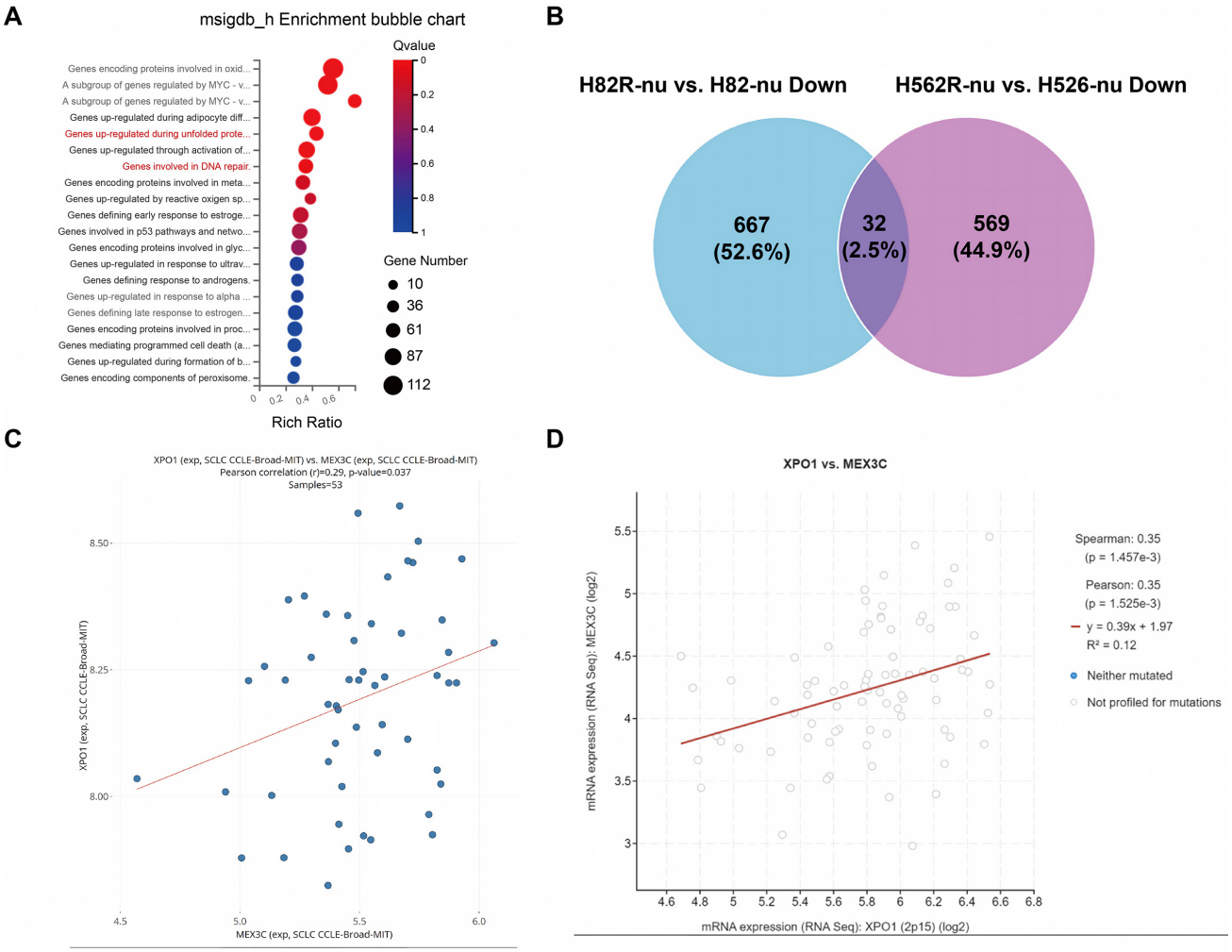


Fig. 2. MEX3C expression correlates with the expression of XPO1 and chemoresistance. (A) Enrichment analysis of up-regulated differentially expressed genes between H82R and H82 cells, as identified by RNA-seq data (N = 3). The full names of the pathways shown have been listed in **Supplementary Table 1**. (B) Venn diagram of differentially expressed nuclear proteins between H82R vs. H82 cells and H526R vs. H526 cells, as identified by proteome sequencing data (N = 3). Correlation analyses of XPO1 mRNA and MEX3C mRNA in the CCLE dataset of SCLC cells (N = 53) using SclcCellMinerCDB (C) and cBioPortal datasets of SCLC patients (N = 81) (D). Nu, nucleus.

the parental cell lines (Fig. 1D). Collectively, these results suggest that XPO1 expression in SCLC tissues may be associated with patient survival and may contribute to chemotherapy resistance in SCLC.

3.2 MEX3C is Associated With Chemotherapy Resistance and XPO1 in SCLC

To further investigate the correlation between XPO1 and chemotherapy resistance in SCLC and to identify potential key molecules, RNA-seq was performed on H82 and H82R cells. Upregulated genes in H82R cells were significantly enriched in the unfolded protein response (UPR) pathway and DNA repair pathways, suggesting a critical role for the nuclear transport protein XPO1 in chemotherapy-resistant SCLC cells (Fig. 2A; **Supplementary Table 1**). Subsequently, iTRAQ-based proteomic analysis was performed on nuclear proteins extracted from H82, H82R, H526, and H526R cells. A total of 699 down-regulated DEPs were identified in H82R vs. H82 cells, and 601 down-regulated DEPs in H526R vs. H526 cells. Among these, 32 overlapping proteins were commonly downregulated in the nuclear proteins of both resistant cell lines (Fig. 2B; **Supplementary Table 2**). Functional annotation of these genes using the NCBI database revealed that among the 23 genes with known functional annotations, three were implicated in protein transport with the keywords “trafficking“ and “shuttle”. Notably, MEX3C was the only annotated nuclear shuttling protein in our screen. Therefore, we hypothesized that MEX3C acted as a crucial mediator associated with chemotherapeutic responses. XPO1 mediates the translocation of MEX3C to the cytoplasm, where it binds to and promotes the degradation of

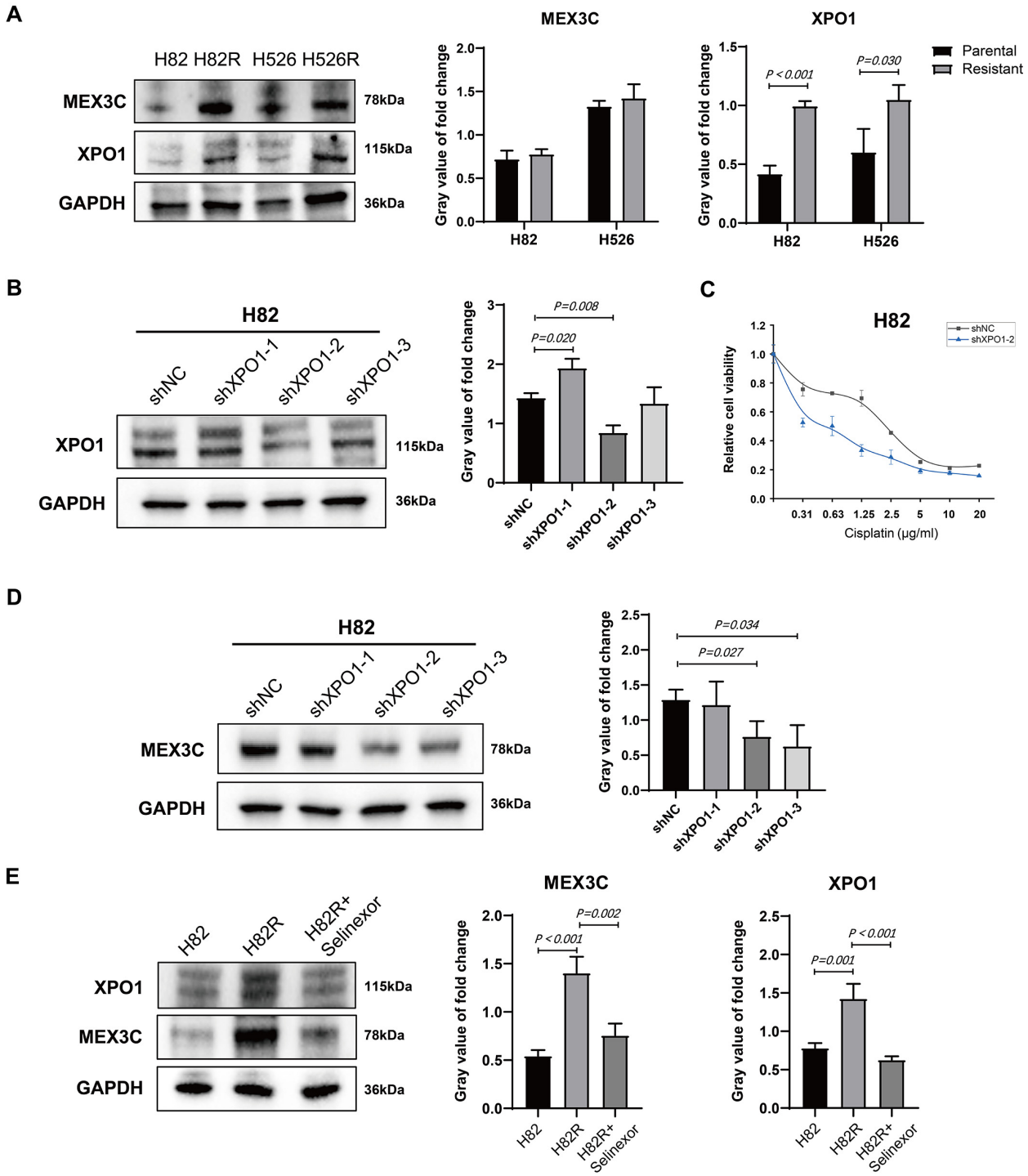


Fig. 3. Correlation of XPO1 expression with MEX3C expression in SCLC cells. (A) Western blot showing protein expression of MEX3C, XPO1 and GAPDH in H82, H82R, H526 and H526R cells. (B) Western blot showing protein expression of XPO1 and GAPDH in H82 cells transfected with shNC, sh*XPO1*-1, sh*XPO1*-2, or sh*XPO1*-3. (C) Relative cell viability of H82 cells transfected with shNC or shXPO1-2, as measured by CCK-8 assay. (D) Western blot showing protein expression of MEX3C and GAPDH in H82 cells transfected with shNC, sh*XPO1*-1, sh*XPO1*-2, or sh*XPO1*-3. (E) Western blot showing protein expression of XPO1, MEX3C, and GAPDH in H82, H82R or Selinexor-treated (0.15 μM) H82R cells. $n = 3$ for biological duplication. shNC, shRNA negative control.

mRNAs encoding cell death-related proteins, thereby inhibiting cell death and contributing to drug resistance. To explore the relationship between XPO1 and MEX3C, we analyzed CCLE and cBioPortal RNA-seq data. The results demonstrated significant positive correlations between *XPO1* and *MEX3C* expression levels in both SCLC cell

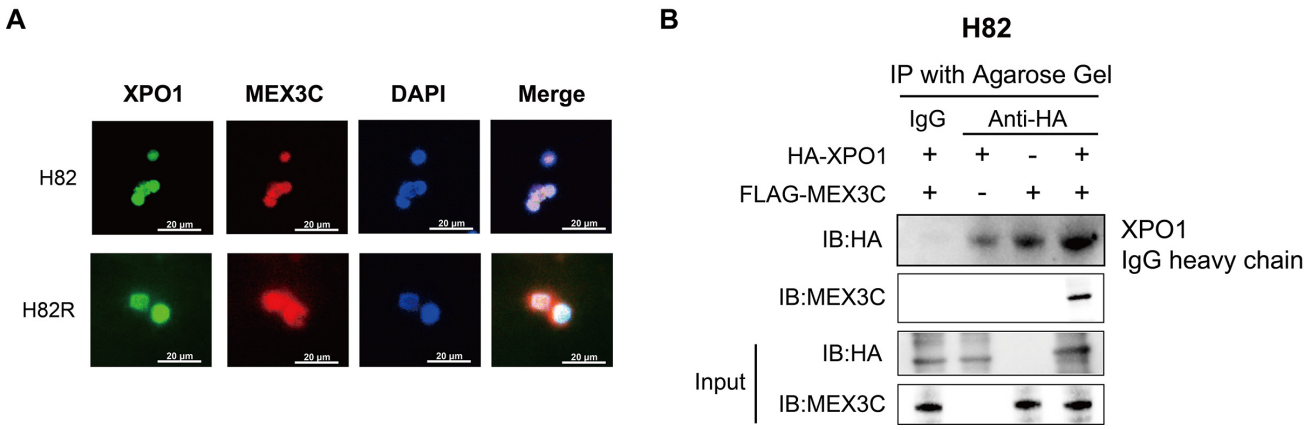


Fig. 4. MEX3C binds to XPO1 in SCLC cells. (A) Immunofluorescence demonstrating the co-localization of MEX3C and XPO1 in H82 and H82R cells. Scale bar = 20 μm. (B) The binding of MEX3C to XPO1 in H82 cells was detected by HA-tagged co-immunoprecipitation and Western blotting. $n = 3$ for biological replicates. IP, immunoprecipitation; HA, hemagglutinin; IB, immunoblotting.

lines (N = 53, $p = 0.037$) (Fig. 2C) and SCLC tumor tissues (N = 81, $p = 0.0015$) (Fig. 2D). These findings suggest that MEX3C may serve as a key regulatory molecule in chemotherapy resistance in SCLC.

3.3 XPO1 Expression Correlates With MEX3C Expression in SCLC Cells

To further investigate the relationship between XPO1 and MEX3C, we examined their expression levels in chemotherapy-resistant SCLC cell lines. Both H82R and H526R cells showed higher levels of XPO1 expression compared to their respective parental cell lines (Fig. 3A). XPO1 expression was significantly reduced in H82 cells following knockdown with *XPO1*-specific shRNA 2 (sh*XPO1*-2) (Fig. 3B). Notably, *XPO1* knockdown markedly increased the sensitivity of H82 cells to cisplatin ($F = 46.30$, $p < 0.0001$) (Fig. 3C). Furthermore, MEX3C expression was also downregulated upon *XPO1* knockdown (Fig. 3D). Consistent with these observations, treatment of H82R cells with the XPO1 inhibitor Selinexor for 48 h resulted in concurrent downregulation of both XPO1 and MEX3C expression (Fig. 3E). Together, these findings indicate that XPO1 expression correlates with MEX3C expression in SCLC cells.

3.4 XPO1 and MEX3C in the Nucleus of SCLC Cells

To further demonstrate the relationship between XPO1 and MEX3C, immunofluorescence staining was performed to visualize the subcellular localization of XPO1 and MEX3C in H82 and H82R cells. Co-localization of XPO1 and MEX3C was observed in the nucleus of SCLC cells (Fig. 4A). Similar co-localization was observed in H526 and H526R cells (**Supplementary Fig. 1**). Furthermore, Co-IP using an anti-HA antibody revealed an interaction between XPO1 and MEX3C proteins in H82 cells (Fig. 4B). Collectively, these findings indicate that XPO1 may interact with MEX3C in the nucleus of SCLC cells.

3.5 Combined Inhibition of XPO1 and MEX3C Suppresses the Proliferation of Platinum-Resistant SCLC Cells

We first evaluated the effects of different XPO1 inhibitors on SCLC cell proliferation. Treatment with XPO1 inhibitors, including Selinexor, WJ01075, and WJ01024, significantly suppressed the proliferation of SCLC cells in a dose-dependent manner (Fig. 5A–C). These agents are currently being investigated in clinical studies for SCLC chemotherapy [17]. To determine whether concurrent targeting of XPO1 and MEX3C enhances the anti-proliferative effects, we treated H82R cells with the XPO1 inhibitor Selinexor in combination with sh*MEX3C*. This combination treatment significantly inhibited H82R cell proliferation compared to Selinexor treatment alone (Fig. 5D, **Supplementary Fig. 2**). Collectively, the results suggest that simultaneous inhibition of XPO1 and MEX3C can suppress SCLC cell growth.

4. Discussion

The regulatory mechanism of XPO1 in SCLC currently remains unclear, and its relationship with chemotherapy resistance in SCLC has yet to be definitively established. This study found that high XPO1 expression in SCLC was associated with chemotherapy resistance. Mechanistically, XPO1 may facilitate chemoresistance by binding to the shuttling protein MEX3C and mediating its translocation to the cytoplasm. Simultaneous inhibition of XPO1 and MEX3C was observed to significantly suppress the growth of chemotherapy-resistant SCLC cells. Collectively, these findings provide a theoretical basis for the development of novel combination therapies and individualized treatment strategies for SCLC.

Although the relationship between XPO1 and chemoresistance in SCLC has not yet been fully elucidated, in colorectal cancer the XPO1 inhibitor KPT-330 was reported to reverse oxaliplatin resistance via nuclear retention of p53 [18]. The efficacy of chemotherapy is

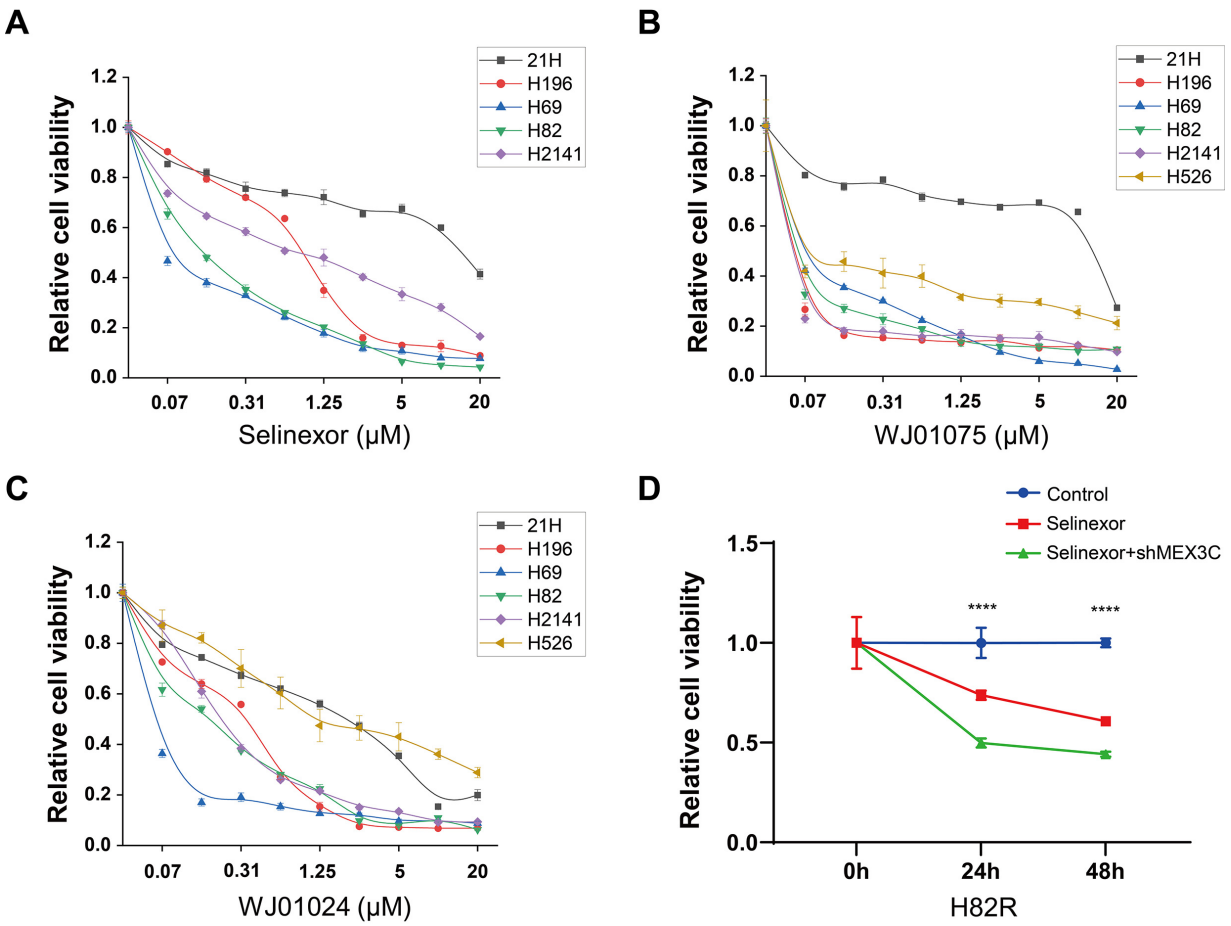


Fig. 5. Concurrent inhibition of XPO1 and MEX3C inhibits the growth of chemotherapy-resistant SCLC cells. (A–C) Relative cell viability of SCLC cells treated with Selinexor (A), WJ01075 (B), and WJ01024 (C), as assessed by CCK-8 assay. (D) Relative cell viability of H82R cells treated with Selinexor (0.15 μM) or Selinexor combined with sh*MEX3C*, as measured by CCK-8 assay. $n = 3$ for biological duplication. ****$p < 0.0001$.

well-recognized in both colorectal cancer and SCLC. However, platinum-based drug resistance remains a major challenge. Consistent with our findings, XPO1 has previously been associated with chemoresistance in both colorectal cancer and SCLC, with XPO1 inhibitors shown to reverse this resistance. Similarly, XPO1 inhibitors have been shown to exert potent anti-tumor effects in triple-negative breast cancer [19]. XPO1 has also been identified as a key regulator of paclitaxel resistance in ovarian cancer [20]. Beyond solid tumors, XPO1 has been implicated in mediating drug resistance in lymphoma [21,22]. The findings of the present study indicate that XPO1 is significantly associated with chemoresistance in SCLC, highlighting its critical role in this refractory cancer. Notably, XPO1 resolved into two distinct bands in our Western blotting experiments, in agreement with prior literature [23]. This band heterogeneity originates from alternatively spliced XPO1 isoforms that yield proteins of varying molecular weights [24].

Our investigation also revealed that MEX3C, a member of the MEX-3 RNA-binding protein family, may serve as a key molecule through which XPO1 regulates chemotherapy resistance in SCLC. MEX3C regulates gene expression post-transcriptionally by targeting specific mRNAs for degradation or stabilization via its ubiquitin ligase activity [25,26]. Mutations in MEX3C contribute to chromosomal instability, a key driver of colorectal cancer [27], and its dysregulation has been implicated in immune regulation, cell differentiation, and metabolism [26,28]. In non-small cell lung cancer (NSCLC), MEX3C overexpression contributes to poor prognosis by influencing immune infiltration and the tumor microenvironment [25]. However, the role of MEX3C in SCLC remains poorly understood.

Through RNA-seq and proteomic profiling, our screening identified MEX3C as the only downregulated shuttling protein in the nuclear fraction of chemotherapy-resistant SCLC cells compared to parental cells. Moreover, we demonstrated the interaction of MEX3C with XPO1 in SCLC cells, alongside the cytoplasmic accumulation of MEX3C in chemotherapy-resistant cells. Consistent with our findings, a previous study reported that MEX3C functions as an adaptor protein for XPO1-mediated nuclear ex-

port in mouse ovaries [29]. Beyond its role as an RNA-binding protein [29], the interaction between MEX3C and XPO1 may also contribute to chemoresistance in SCLC. In cervical cancer, inhibition of MEX3C has been shown to significantly reduce cell proliferation, invasion, sphere formation, and paclitaxel resistance [30], in line with our observation that MEX3C is associated with chemoresistance in SCLC.

By integrating information from publicly available databases on SCLC patients and cell lines, along with *in vitro* cellular experiments and multi-omics analyses, this study confirmed the association between XPO1 and chemoresistance in SCLC. More importantly, we identified MEX3C as a key molecule through which XPO1 regulates chemoresistance in SCLC, and demonstrated that MEX3C may serve as a potential co-therapeutic target for XPO1-based therapy. Our findings fill a critical gap in understanding the roles of XPO1 and MEX3C in SCLC drug resistance, while also providing a novel combinatorial strategy for XPO1-targeted therapy. Additionally, both MEX3C and XPO1 may serve as potential biomarkers for chemoresistance.

5. Limitation

Nevertheless, several limitations of this study should be acknowledged. Our experiments were conducted exclusively *in vitro* using SCLC cell lines, and no *in vivo* studies (e.g., animal models or organoid cultures) were performed. Moreover, the downstream signaling pathways regulated by the XPO1/MEX3C axis have yet to be fully elucidated. We conducted only loss-of-function experiments to confirm the role of the XPO1-MEX3C axis in chemotherapy resistance. The absence of overexpression and rescue complementation experiments to verify sufficiency represents a limitation of this study. Future work will further characterize the relationship between XPO1 and MEX3C using *in vivo* assays. We will also conduct SCLC subtype identification and subtype-specific analyses, and uncover additional potential therapeutic targets in the regulatory network to extend our investigation of the XPO1-MEX3C regulatory axis, which should provide additional evidence of their roles in chemoresistance, thereby advancing personalized and precision medicine for SCLC with the ultimate goal of prolonging patient survival.

6. Conclusions

XPO1 is upregulated in chemotherapy-resistant SCLC and correlates with the expression of MEX3C. XPO1 interacts with MEX3C in the nucleus, and their combined inhibition suppresses the growth of platinum-resistant SCLC cells. Collectively, these findings help to elucidate the mechanism by which XPO1 and MEX3C regulate chemotherapy resistance in SCLC and may provide new insights into combination therapy for this malignancy.

Abbreviations

XPO1, exportin-1; SCLC, small-cell lung cancer; CRM1, chromosome region maintenance 1; SINE, selective inhibitors of nuclear export; FDA, Food and Drug Administration; FOXO3a, Forkhead box O3a; HDAC, histone deacetylase; CCK-8, Cell Counting kit-8; DEPs, differentially expressed proteins; shRNAs, short hairpin RNAs; BSA, bovine serum albumin; SD, standard deviation; OS, overall survival; PFS, progression-free survival; UPR, unfolded protein response; Co-IP, co-immunoprecipitation; NSCLC, non-small cell lung cancer.

Availability of Data and Materials

The data that support the findings of this study are available from the corresponding authors upon reasonable request.

Author Contributions

PYZ: project administration, formal analysis, supervision, writing - original draft, writing - review and editing. SZ: conceptualization, data curation, formal analysis, visualization, writing - review and editing. XYW: formal analysis, supervision, visualization, writing - review and editing. HRC: formal analysis, methodology, validation, writing - review and editing. YHL: formal analysis, methodology, data curation, writing - review and editing. HL: formal analysis, project administration, supervision, writing - review and editing. HFL: conceptualization, funding acquisition, project administration, writing - review and editing. All authors contributed to editorial changes in the manuscript. All authors read and approved the final manuscript. All authors have participated sufficiently in the work and agreed to be accountable for all aspects of the work.

Ethics Approval and Consent to Participate

Not applicable.

Acknowledgment

We are grateful to Prof. Hongbin Ji for generously providing the cell lines used in this study.

Funding

This research was funded by Jilin Provincial Department of Science and Technology (YDZJ202301ZYTS515).

Conflicts of Interest

The authors declare no conflicts of interest.

Supplementary Material

Supplementary material associated with this article can be found, in the online version, at https://doi.org/10.31083/FBL55654.

References

[1] Zhang S, Li H, Zhao P, Yao J, Cheng Y. Targeting XPO1: A new perspective for malignant solid tumor especially small cell lung cancer. Chinese Medical Journal. 2026; 139: 148–150. https://doi.org/10.1097/CM9.0000000000003654

[2] Li YQ, Fang Z, Zhang W, Rao GW, Zheng Q. Targeting XPO1 for fighting relapsed/refractory diseases: The research progress of XPO1 inhibitors. Bioorganic Chemistry. 2025; 154: 108073. https://doi.org/10.1016/j.bioorg.2024.108073

[3] Azmi AS, Uddin MH, Mohammad RM. The nuclear export protein XPO1 - from biology to targeted therapy. Nature Reviews. Clinical Oncology. 2021; 18: 152–169. https://doi.org/10.1038/s41571-020-00442-4

[4] Yang Y, Guo L, Chen L, Gong B, Jia D, Sun Q. Nuclear transport proteins: structure, function, and disease relevance. Signal Transduction and Targeted Therapy. 2023; 8: 425. https://doi.org/10.1038/s41392-023-01649-4

[5] Chen YF, Adams DJ. Therapeutic targeting of exportin-1 beyond nuclear export. Trends in Pharmacological Sciences. 2025; 46: 20–31. https://doi.org/10.1016/j.tips.2024.11.002

[6] Kalakonda N, Maerevoet M, Cavallo F, Follows G, Goy A, Vermaat JSP, et al. Selinexor in patients with relapsed or refractory diffuse large B-cell lymphoma (SADAL): a single-arm, multinational, multicentre, open-label, phase 2 trial. The Lancet. Haematology. 2020; 7: e511–e522. https://doi.org/10.1016/S2352-3026(20)30120-4

[7] Kasamon YL, Price LSL, Okusanya OO, Richardson NC, Li RJ, Ma L, et al. FDA Approval Summary: Selinexor for Relapsed or Refractory Diffuse Large B-Cell Lymphoma. The Oncologist. 2021; 26: 879–886. https://doi.org/10.1002/onco.13859

[8] Kim SY, Park HS, Chiang AC. Small Cell Lung Cancer: A Review. JAMA. 2025; 333: 1906–1917. https://doi.org/10.1001/jama.2025.0560

[9] Sen T, Takahashi N, Chakraborty S, Takebe N, Nassar AH, Karim NA, et al. Emerging advances in defining the molecular and therapeutic landscape of small-cell lung cancer. Nature Reviews. Clinical Oncology. 2024; 21: 610–627. https://doi.org/10.1038/s41571-024-00914-x

[10] Qin T, Wang J, Wang J, Du Q, Wang L, Liu H, et al. Nuclear to Cytoplasmic Transport Is a Druggable Dependency in HDAC7-driven Small Cell Lung Cancer. Advanced Science (Weinheim, Baden-Wurttemberg, Germany). 2025; 12: e2413445. https://doi.org/10.1002/advs.202413445

[11] Wang J, Sun T, Meng Z, Wang L, Li M, Chen J, et al. XPO1 inhibition synergizes with PARP1 inhibition in small cell lung cancer by targeting nuclear transport of FOXO3a. Cancer Letters. 2021; 503: 197–212. https://doi.org/10.1016/j.canlet.2021.01.008

[12] Jiang Y, Xing D, He X, Wu W, Xu H, Sun H, et al. Targeting EP300 in diffuse large b-cell lymphoma: efficacy of A485 and synergistic effects with XPO1 inhibition. BMC Cancer. 2025; 25: 955. https://doi.org/10.1186/s12885-025-14257-y

[13] Totiger TM, Chiraphapphaiboon W, Baca Y, Chaudhry S, Notti RQ, Montoya S, et al. XPO1 R749Q Mutations Co-occur with POLE Mutations in Cancer and Can Be Targeted to Overcome Chemoresistance. Cancer Research. 2025; 85: 3219–3233. https://doi.org/10.1158/0008-5472.CAN-24-3112

[14] Kruer TL, Quintana A, Newman H, Ferrall-Fairbanks M, Zhang L, McLemore A, et al. XPO1 drives resistance to eprenetapopt and azacitidine and can be targeted in TP53-mutated myeloid malignancies. Blood. 2025; 146: 2244–2258. https://doi.org/10.1182/blood.2025028803

[15] George J, Lim JS, Jang SJ, Cun Y, Ozretić L, Kong G, et al. Comprehensive genomic profiles of small cell lung cancer. Nature. 2015; 524: 47–53. https://doi.org/10.1038/nature14664

[16] Wei Y, Gao Z, Qi B, Wu Y, Chen J. High expression of YKT6 promotes lung cancer cell proliferation and inhibits autophagy. Holistic Integrative Oncology. 2026; 5: 24. https://doi.org/10.1007/s44178-026-00240-5

[17] Quintanal-Villalonga A, Taniguchi H, Hao Y, Chow A, Zhan YA, Chavan SS, et al. Inhibition of XPO1 sensitizes small cell lung cancer to first- and second-line chemotherapy. Cancer Research. 2022; 82: 472–483. https://doi.org/10.1158/0008-5472.CAN-21-2964

[18] Lai C, Jia X, Chen Y, Chen K, Wang F, Zhang Q, et al. Exportin 1 inhibitor KPT-330 reverses oxaliplatin resistance via p53 nuclear retention in colorectal cancer. International Journal of Molecular Medicine. 2026; 57: 4. https://doi.org/10.3892/ijmm.2025.5675

[19] Rashid NS, Hairr NS, Murray G, Olex AL, Leftwich TJ, Grible JM, et al. Identification of nuclear export inhibitor-based combination therapies in preclinical models of triple-negative breast cancer. Translational Oncology. 2021; 14: 101235. https://doi.org/10.1016/j.tranon.2021.101235

[20] Fan M, Liu K, Shi Y, Hao J, Qiu H, Liang Y. N4BP3 promotes ovarian cancer progression and paclitaxel resistance by activating the Wnt/β-catenin signaling through interaction with XPO1. Experimental Cell Research. 2025; 452: 114751. https://doi.org/10.1016/j.yexcr.2025.114751

[21] Xu Y, Wang L, He C, Liu Z, Fu R, Xie Y. NAT10 Mediates XPO1 mRNA N4-acetylation and Promotes Drug Resistance of Myeloma Cells. Journal of Cancer. 2024; 15: 6355–6363. https://doi.org/10.7150/jca.101403

[22] Chanukuppa V, Paul D, Taunk K, Chatterjee T, Sharma S, Kumar S, et al. XPO1 is a critical player for bortezomib resistance in multiple myeloma: A quantitative proteomic approach. Journal of Proteomics. 2019; 209: 103504. https://doi.org/10.1016/j.jprot.2019.103504

[23] Wang J, Chen M, Jiang J, Wan Y, Li X, Zhang M, et al. Targeting deubiquitinase USP7-mediated stabilization of XPO1 contributes to the anti-myeloma effects of selinexor. Journal of Translational Medicine. 2025; 23: 62. https://doi.org/10.1186/s12967-025-06068-3

[24] Chaudhry S, Beckedorff F, Jasdanwala SS, Totiger TM, Affer M, Lawal AE, et al. Altered RNA export by SF3B1 mutants confers sensitivity to nuclear export inhibition. Leukemia. 2024; 38: 1894–1905. https://doi.org/10.1038/s41375-024-02328-1

[25] Zhang M, Cao L, Hou G, Lv X, Deng J. Investigation of the Potential Correlation Between RNA-Binding Proteins in the Evolutionarily Conserved MEX3 Family and Non-small-Cell Lung Cancer. Molecular Biotechnology. 2023; 65: 1263–1274. https://doi.org/10.1007/s12033-022-00638-2

[26] Xiao Y, Li Y, Shi D, Wang X, Dai S, Yang M, et al. MEX3C-Mediated Decay of SOCS3 mRNA Promotes JAK2/STAT3 Signaling to Facilitate Metastasis in Hepatocellular Carcinoma. Cancer Research. 2022; 82: 4191–4205. https://doi.org/10.1158/0008-5472.CAN-22-1203

[27] Burrell RA, McClelland SE, Endesfelder D, Groth P, Weller MC, Shaikh N, et al. Replication stress links structural and numerical cancer chromosomal instability. Nature. 2013; 494: 492–496. https://doi.org/10.1038/nature11935

[28] Lu P, Li H, Li N, Singh RN, Bishop CE, Chen X, et al. MEX3C interacts with adaptor-related protein complex 2 and involves in miR-451a exosomal sorting. PloS One. 2017; 12: e0185992. https://doi.org/10.1371/journal.pone.0185992

[29] Li X, Li Y, Liu C, Jin M, Lu B. Oocyte-Specific Expression of Mouse MEX3C652AA in the Ovary and Its Potential Role in Regulating Maternal Fos mRNA. Biology of Reproduction. 2016; 94: 115. https://doi.org/10.1095/biolreprod.115.136630

[30] Yi H, Han Y, Li Q, Wang X, Xiong L, Li S. Circular RNA circ_0004488 Increases Cervical Cancer Paclitaxel Resistance via the miR-136/MEX3C Signaling Pathway. Journal of Oncology. 2022; 2022: 5435333. https://doi.org/10.1155/2022/5435333